

Spatiotemporal changes of normalized difference vegetation index (NDVI) and response to climate extremes and ecological restoration in the Loess Plateau, China

Anzhou Zhao^{1,2} · Anbing Zhang^{1,2} · Xianfeng Liu³ · Sen Cao⁴

Received: 21 December 2016 / Accepted: 21 March 2017 / Published online: 30 March 2017
© Springer-Verlag Wien 2017

Abstract Extreme drought, precipitation, and other extreme climatic events often have impacts on vegetation. Based on meteorological data from 52 stations in the Loess Plateau (LP) and a satellite-derived normalized difference vegetation index (NDVI) from the third-generation Global Inventory Modeling and Mapping Studies (GIMMS3g) dataset, this study investigated the relationship between vegetation change and climatic extremes from 1982 to 2013. Our results showed that the vegetation coverage increased significantly, with a linear rate of 0.025/10a ($P < 0.001$) from 1982 to 2013. As for the spatial distribution, NDVI revealed an increasing trend from the northwest to the southeast, with about 61.79% of the LP exhibiting a significant increasing trend ($P < 0.05$). Some temperature extreme indices, including TMAXmean, TMINmean, TN90p, TNx, TX90p, and TXX, increased significantly at rates of 0.77 mm/10a, 0.52 °C/10a, 0.62 °C/10a, 0.80 °C/10a, 5.16 days/10a, and 0.65 °C/10a, respectively. On the other hand, other extreme temperature indices including TX10p and TN10p decreased significantly at rates of

–2.77 days/10a and 4.57 days/10a ($P < 0.01$), respectively. Correlation analysis showed that only TMINmean had a significant relationship with NDVI at the yearly time scale ($P < 0.05$). At the monthly time scale, vegetation coverage and different vegetation types responded significantly positively to precipitation and temperature extremes (TMAXmean, TMINmean, TNx, TNn, TXn, and TXX) ($P < 0.01$). All of the precipitation extremes and temperature extremes exhibited significant positive relationships with NDVI during the spring and autumn ($P < 0.01$). However, the relationship between NDVI and RX1day, TMAXmean, TXn, and TXX was insignificant in summer. Vegetation exhibited a significant negative relationship with precipitation extremes in winter ($P < 0.05$). In terms of human activity, our results indicate a strong correlation between the cumulative afforestation area and NDVI in Yan'an and Yulin during 1998–2013, $r = 0.859$ and 0.85 , $n = 16$, $P < 0.001$.

1 Introduction

Extreme climatic events are defined as significant statistical deviations for certain climatic factors that meet or exceed specific lower and upper limit threshold statistical or observed values (Zheng et al. 2014). The Fifth Intergovernmental Panel on Climate Change Assessment Report (IPCCAR5) shows that the globally averaged temperature increased by 0.85 °C (0.65 to 1.06 °C) over the period from 1880 to 2012 (Liao and Chang 2014). There is a general agreement that global warming may have enhanced the intensity, frequency, and severity of extreme climatic events over the past century (Wallace et al. 2014). Compared with average climate trends, extreme climatic events (e.g., floods and droughts) are often unusual and unpredictable and would have significant impacts on human societies and natural ecosystems (Liu et al. 2015a,

✉ Anzhou Zhao
zhaozhou@126.com

✉ Anbing Zhang
zhangbing@hebeu.edu.cn

¹ School of Mining and Geomatics, Hebei University of Engineering, Handan 056038, Hebei, People's Republic of China

² Hebei Collaborative Innovation Center of the Comprehensive Development and Utilization of Coal Resource, 199 Guangming Street, Handan 056038, People's Republic of China

³ College of Tourism and Environment, Shaanxi Normal University, Xi'an, Shaanxi 710062, People's Republic of China

⁴ Department of Earth and Atmospheric Sciences, University of Alberta, Edmonton T6G 2E3, Canada

b). With an increase in the extreme climatic events under future climate change, knowledge of their patterns, structure, and processes in terrestrial ecosystem, especially vegetation responses to extreme events, must be understood (Seneviratne et al. 2012). Therefore, by analyzing vegetation change trends and response to extreme climatic events, we can improve our understanding of vegetation vulnerability to climate fluctuations.

With increasing interest about global climate change, there is much concern about the relationship between vegetation growth and climate change (Miao et al. 2012; Zhang et al. 2016a, b). The effects of climate change (e.g., trend, fluctuation, and extreme events) on vegetation growth are diverse (Tan et al. 2015). There are numerous studies that focus on the change in vegetation coverage due to trends and fluctuations in climate (Piao et al. 2011; Sun et al. 2015a, b), but few of them have discussed the impact of extreme climatic events on vegetation growth (Liu et al. 2016). Recently, some researchers have studied the relationship between vegetation and extreme climate conditions. For example, John et al. (2013) assessed the response of vegetation (grassland and desert biome) to extreme climate events on the Mongolian Plateau from 2000 to 2010 and showed that the desert biome is more vulnerable than the grassland biome in dry years. Hilker et al. (2014) studied the sensitivity of vegetation dynamics to rainfall and El Niño events. Their results indicated that there is a close relationship between vegetation growth, annual precipitation, and El Niño events in the Amazon rainforest. Liu et al. (2013) assessed vegetation extremes and sensitivity to climate extremes at a global scale from 1982 to 2006 and showed that severe precipitation extremes have a clear correlation with declines in temperate broadleaf forest and temperate grassland. In China, studies about vegetation response to extreme climatic events, especially in vulnerable ecological regions such as the Loess Plateau (LP), are few. IPCCAR5 documented that the atmospheric temperature increased by 1.38 °C from 1960 to 2009 in China. This rate of increase is greater than the global value (i.e., 0.72 °C from 1951 to 2012) (Stocker 2013). A rapid increase in temperature is likely to lead to an increase in the intensity, frequency, and severity of extreme climatic events (Reichstein et al. 2013). Extreme climatic events not only affect vegetation coverage, but also alter the relationship between vegetation features and climatic (Liu et al. 2016). Thus, it is necessary to assess vegetation coverage and its relationship with extreme climatic events in extremely vulnerable regions of China.

Since the early twenty-first century, a series of policies such as the Grain to Green Program (GGP) and the Grazing Withdrawal Program have been launched in the sensitive and fragile ecological regions of China (Lü et al. 2015). The effects of such policies became a major concern of society. The LP, which is located in the middle reaches of the Yellow River, is dominated by cultivated vegetation, forest, and

grassland (Xiao 2014). The region not only is pilot region of the ecological engineering construction projects, but also is a fragile ecological environment that is sensitive to climate change (Xiao 2014). The LP has attracted much research attention because of extreme soil and water loss, as well as implementation of the GGP over the past decades when climate conditions and anthropogenic activities with the LP changed dramatically (Xin et al. 2008; Zhang et al. 2013a, b; Sun et al. 2015a, b). From 1951 to 2008, temperature increased at a rate of 0.02 °C/a and rainfall decreased at a rate of 0.97 mm/a (Lü et al. 2012). Because the GGP was implemented in the LP in 1999, 16,000 km² of rain-fed cropland was converted to planted vegetation from 2000 to 2010 (Feng et al. 2016). Previous studies have indicated that the number of extreme climatic events increased during that time, and precipitation, temperature, and human activities had important impacts on vegetation coverage in the LP (Li et al. 2010; Sun et al. 2016). However, few studies have been conducted to quantitatively analyze the relationship between vegetation growth and extreme climatic events in the LP, especially when it comes to analyzing the relationships of different vegetation types with extreme climatic events.

In this context, this study attempts to analyze the spatio-temporal changes of vegetation cover and response to extreme climatic events in the LP from 1982 to 2013. The specific objectives of this study are to (1) assess spatiotemporal changes of vegetation in the LP from 1982 to 2013; (2) quantitatively analyze the changing trend of extreme climatic events in the LP from 1982 to 2013; and (3) investigate the relationships between vegetation coverage, vegetation types, and extreme climatic events and ecological restoration activities.

2 Materials and methods

2.1 Study area

The LP is located in the middle reaches of the Yellow River, North China (104°54′–114°33′E, 33°43′–41°16′N), and covers an area of approximately 624,000 km². The TaiHang Mountains, RiYue Mountain, QinLing Mountains, and Yin Mountain are situated to the east, west, south, and north of the LP, respectively (Fig. 1). This region is dominated by a temperate continental monsoon climate, and the average annual precipitation ranges from 150 mm/a in the northwest to 800 mm/a in the southeast. The annual precipitation of 55 to 78% occurs between June and September in the form of rainstorms (Liu et al. 2016). The annual average temperature ranges from 4.3 °C in the northwest to 14.3 °C in the southeast. The total solar heat gain and annual average sunshine are 5.0–6.3 × 10⁹ J/m² and 2200–2800 h. Potential evaporation ranges from 865 to 1274 mm (Li et al. 2012). From the northwest to the southeast, the main soil types change from eolian

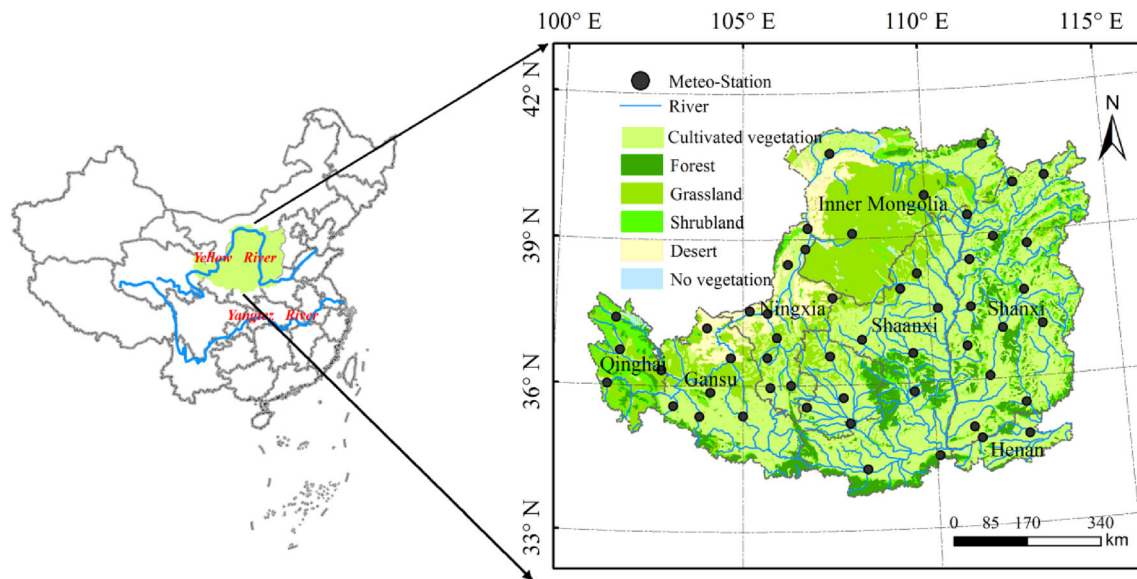


Fig. 1 Distribution of meteorological stations and vegetation types in LP, China

sand and sandy loess to typical loess and clayey loess. The dominant vegetation types include cultivated vegetation, artificial forest, rangeland, shrub land, and grassland (Xiao 2014). The uneven distribution of water availability, climate variability, and extensive human activities has resulted in drought hazards, severe soil erosion, and desertification in the LP.

2.2 Data

The GIMMS NDVI3g dataset was downloaded from the NOAA-Advanced Very High Resolution Radiometer (AVHRR) for the period from 1982 to 2013. GIMMS NDVI3g has a spatial resolution of $1/12^\circ$ and a temporal resolution of 15 days (Fensholt and Proud 2012; Guay et al. 2014). The GIMMS NDVI3g dataset has been optimized to minimize the effects of the differences in sensor design between the AVHRR/2 and AVHRR/3 instruments as well as volcanic eruptions (Pinzon and Tucker 2014; Liu et al. 2015a, b). The monthly GIMMS NDVI3g dataset was calculated by using maximum value composite (MVC) technique, and the maximum annual NDVI was calculated to detect the spatiotemporal variation of vegetation in the LP. A vegetation map of the LP was digitized from a 1:1,000,000 scale map of vegetation in China (Hou 2001). Vegetation types in the LP include needle-leaf forest, broad-leaved forest, shrub land, cultivated vegetation, steppe, meadow, marshy grassland, and desert. In this study, we focused on cultivated vegetation, forest (needle-leaf forest and broad-leaved forest), grassland (steppe, meadow, and marshy grassland), and shrub land. In addition, meteorological data (daily maximum air temperature, daily minimum air temperature, and daily precipitation) from 53 meteorological stations were downloaded from the

China Meteorological Data Sharing Service System (<http://data.cma.cn/>) for the period of 1982 to 2013. It should be noted that the NDVI value for each meteorological station was calculated as the mean value of its 3×3 neighbors.

In this study, 12 indices of extreme climate events (2 precipitation indices and 10 temperature indices) (Zhang et al. 2005) were selected to analyze extreme climate changes in the LP (Table 1). Extreme climate indices were generated by the Commission for Climatology (CCI)/Climate Variability and Predictability (CLIVAR)/Joint WMO-IOC Technical Commission for Oceanography and Marine Meteorology (JCOMM) Expert Team (ET) on Climate Change Detection and Indices (ETCCDI) (<http://ccma.seos.uvic.ca/ETCCDI>) (You et al. 2011). The indices were calculated by the RClimDex software and widely used in the study of extreme climate events. The indices were calculated by the RClimDex software. Values for daily maximum air temperature, daily minimum air temperature, and daily precipitation data have been quality controlled.

2.3 Methodology

The metrics of Theil–Sen (TS) median slope and Mann–Kendall (MK) were used to detect the change trends and significance of the trend in NDVI and climate extremes time series during 1982–2013 (Stow et al. 2003). The noise with parametric uncertainty present in the regression equation can be avoided by TS-MK method. The slope is calculated as follows:

$$\text{Slope} = \text{Median} \frac{\text{NDVI}_j - \text{NDVI}_i}{t_j - t_i} \quad (1)$$

Table 1 Descriptions of selected precipitation and temperature indices

Index	Descriptive name	Definitions	Unit
RX1day	Max 1-day precipitation amount	Monthly maximum 1-day precipitation	mm
RX5day	Max 5-day precipitation amount	Monthly maximum 5-day precipitation	mm
TMAXmean	Daytime temperature	Monthly mean value of daily maximum temperature	°C
TMINmean	Nocturnal temperature	Monthly mean value of daily minimum temperature	°C
TN10p	Cold nights	Percentage of days when TN < 10th percentile	Days
TN90p	Warm nights	Percentage of days when TN > 90th percentile	Days
TNn	Min Tmin	Monthly minimum value of daily minimum temperature	°C
TNx	Max Tmin	Monthly maximum value of daily minimum temperature	°C
TX10p	Cool days	Percentage of days when TX < 10th percentile	Days
TX90p	Warm days	Percentage of days when TX > 90th percentile	Days
TXn	Min Tmax	Monthly minimum value of daily maximum temperature	°C
TXx	Max Tmax	Monthly maximum value of daily maximum temperature	°C

$$S = \sum_{i=1}^{n-1} \sum_{j=i+1}^n \text{sign}(\text{NDVI}_i - \text{NDVI}_j) \quad (2)$$

$$\text{sign}(\text{NDVI}_i - \text{NDVI}_j) = \begin{cases} -1 & \text{if } (\text{NDVI}_i - \text{NDVI}_j < 0) \\ 0 & \text{if } (\text{NDVI}_i - \text{NDVI}_j = 0) \\ 1 & \text{if } (\text{NDVI}_i - \text{NDVI}_j > 0) \end{cases} \quad (3)$$

$$\text{Var}(S) = \frac{n(n-1)(2n+5)}{18} \quad (4)$$

$$Z = \begin{cases} (S-1)/\sqrt{\text{Var}(S)} & S > 0 \\ 0 & S = 0 \\ (S+1)/\sqrt{\text{Var}(S)} & S < 0 \end{cases} \quad (5)$$

where *Slope* is the trend of NDVI, t_{ij} is the year number, and NDVI_i and NDVI_j are the mean NDVI in the i th and j th year. When *Slope* > 0, the time series of NDVI shows an increasing trend; when *Slope* < 0, the time series of NDVI presents a decreasing trend. If $|Z| > 2.56$, the trend is extremely significant increase or decrease ($P < 0.01$). If $|Z|$ is greater than 1.96 and less than 2.56, the trend is significant increase or decrease ($P < 0.05$). If $|Z|$ is greater than 1.65 and less than 1.96, the trend is weakly significant increase or decrease ($P < 0.1$).

Pearson correlation coefficient was used to calculate the correlations between NDVI and extreme climate indices. It is calculated as follows (Peng et al. 2012):

$$R = \frac{\sum_{i=1}^n (\text{NDVI}_i - \overline{\text{NDVI}}) (P_i - \overline{P})}{\sqrt{\sum_{i=1}^n (\text{NDVI}_i - \overline{\text{NDVI}})^2} \sqrt{\sum_{i=1}^n (P_i - \overline{P})^2}} \quad (6)$$

where R is the Pearson correlation coefficient, NDVI_i and $\overline{\text{NDVI}}$ are the NDVI value in year or month i and the average NDVI value, respectively. P_i and \overline{P} are the value of extreme climate index in year or month i and the average value of extreme climate index.

3 Results

3.1 Temporal variations of vegetation coverage

3.1.1 Variations in annual NDVI

Between 1982 and 2013, the annual NDVI for the LP increased at a rate of 0.025/10a ($P < 0.001$). This rate was much higher than the annual rate for all of China (i.e., 0.002/10a during 1982–2012) (Liu et al. 2015a, b). It also exceeds the increase in growing season for Xinjiang (i.e., 0.003/10a from 1982 to 2012) (Du et al. 2015). From 1982 to 1999, NDVI increased at a rate of 0.017/10a, but the rate of increase from 2000 to 2013 was much higher at 0.08/10a (Fig. 2a). These results show that the implementation of the GGP may have more clear impacts in the LP compared with these other regions.

3.1.2 Temporal variations of different vegetation types

Figure 2b shows the inter-annual NDVI variations for different biomes in the LP. Annual NDVI values from 1982 to 2013 for cultivated vegetation, forest, grassland, and shrub land exhibited significant linear increases in of 0.028/10a, 0.012/10a, 0.027/10a, and 0.02/10a ($P < 0.001$), respectively. Forested vegetation had the highest NDVI values, ranging from 0.7658 to 0.8530. Grasslands had the lowest NDVI values, ranging from 0.3878 to 0.5603.

3.2 Spatial variations of vegetation coverage

3.2.1 General characteristics of NDVI

Generally, annual NDVI values for the LP decreased gradually from southeast to northwest. Low NDVI values were found

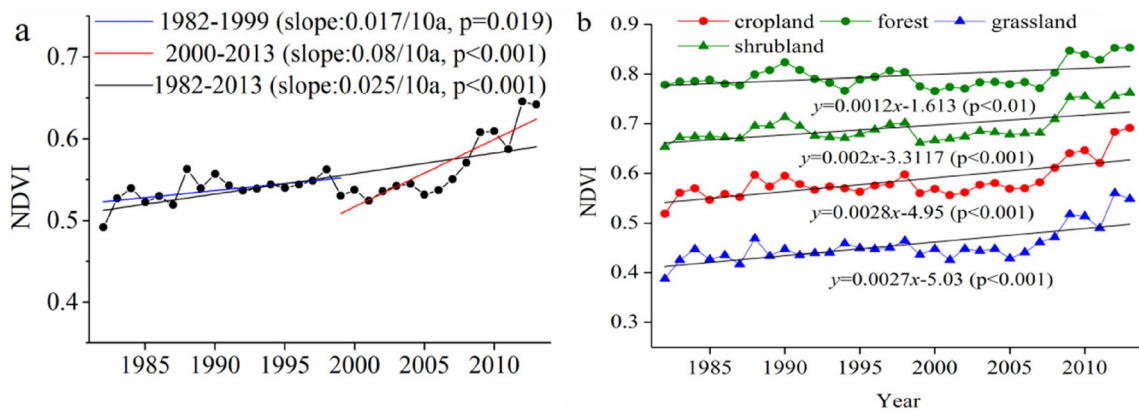


Fig. 2 Interannual variations in NDVI over LP during 1982–2013

in Yulin (Shaanxi); Yike Zhao League (Inner Mongolia); Guyuan and Wuzhong (Ningxia); and Dingxi, Qingyang, and Baiyin (Gansu), primarily because these regions are mainly grassland and desert. High NDVI values were distributed throughout the central and southern regions of Shaanxi because these areas are covered by forest and shrub land (Fig. 3a). We also calculated the frequency histogram for NDVI. Areas with NDVI values greater than 0.5 account for 57.41% of the whole area (Fig. 3b).

3.2.2 NDVI change trend

In order to analyze the NDVI change trend in the LP, we used the TS-MK calculation method. Results showed that the NDVI change trend was highly variable from 1982 to 2013. The NDVI in most areas increased (89.66 vs 10.34%) (Fig. 3c). Areas of highly significant increases, significant increases, and weak significant increases accounted for 49.79, 12.30, and 6.07% of the LP, respectively. By contrast,

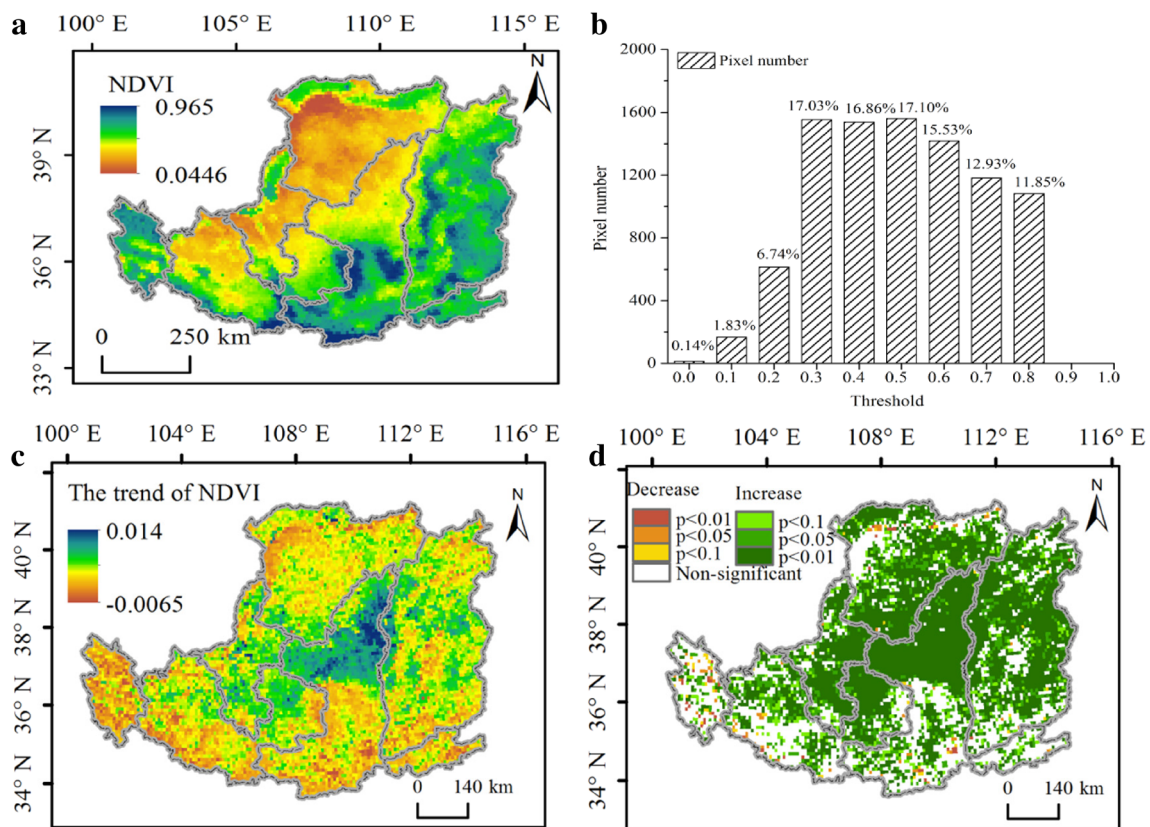


Fig. 3 Spatial distribution, frequency graph, trend, and significance of NDVI in LP during 1982–2013

in 0.58, 0.85, and 0.61% of the LP, NDVI values decreased significantly at the $P = 0.01$, 0.05, and 0.1 levels, respectively. Spatially, areas with significant variation in NDVI were mainly found in the north and middle parts of the region (Fig. 3d).

3.3 Change trends for the climate extreme indices

The variations for the 12 climate extreme indices in the LP from 1982 to 2013 are shown in Fig. 4. The linear trends for RX5day, TMAXmean, TMINmean, TN90p, TNn, TNx, TX90p, and TXx have increased at rates of 0.77 mm/10a, 0.52 °C/10a, 0.62 °C/10a, 8.7 days/10a, 0.01 °C/10a, 0.80 °C/10a, 5.16 days/10a, and 0.65 °C/10a, respectively. Six of the extreme temperature indices (TMAXmean, TMINmean, TN90p, TNx, TX90p, and TXx) all increased significantly at the 0.01 level. By contrast, the linear trends for RX1day, TX10p, TXn, and TN10p decreased at rates of 0.25 mm/10a, 2.77 days/10a, 0.53 °C/10a, and 4.57 days/10a, respectively. Only two extreme temperature indices (TX10p and TN10p) decreased significantly at the 0.01 level.

3.4 Correlation between NDVI and climate extreme indices

Climate change has led to more frequent extreme events that have significant impacts on vegetation cover. Correlations between annual NDVI values and the climate extreme indices were calculated for the LP (Table 2). RX1day, RX5day, TMAXmean, TMINmean, TN90p, TNx, TX90p, and TXx had positive relationships with NDVI. In contrast, TN10p,

TNn, TX10p, and TXn had negative relationships with NDVI. However, only TMINmean exhibited a significant relationship with NDVI ($P < 0.05$). It was shown that temperature increasing at nighttime was greater than daytime in LP (Zhao et al. 2016).

Correlations between NDVI and extreme events have not been found to be significant at the annual scale, indicating that warm or moist weather is not a prerequisite for faster vegetation growth (Liu et al. 2015a, b). In order to understand the relationship between the vegetation cover and extreme events, we analyzed the correlations between NDVI and the 12 climate extreme indices on a monthly basis. The results indicated that RX5day, RX1day, TMAXmean, TMINmean, TNx, TNn, TXn, and TXx had a dominant effect on the NDVI, while TN10, TN90, TX10p, and TX90p did not. Correlations between NDVI and RX5day, RX1day, TMAXmean, TMINmean, TNx, TNn, TXn, and TXx were significant ($P < 0.01$) (Fig. 5). Monthly NDVI values generally responded positively to extreme precipitation and temperature index values. It was indicated that the change trend of NDVI is similar to extreme precipitation and temperature.

Because TN10p, TN90p, TX10p, and TX90p had non-significant relationships with NDVI at the monthly time scale, certain extreme temperature indices (TMAXmean, TMINmean, TNn, TNx, TXn, and TXx) and extreme precipitation indices (RX1day and RX5day) were selected to represent typical extreme climate indices. At the biome scale, different biomes to extreme precipitation and temperature indices were also detected (Table 3). For example, 65, 65, 66, and 62% of the vegetation dynamics in grassland, shrub land,

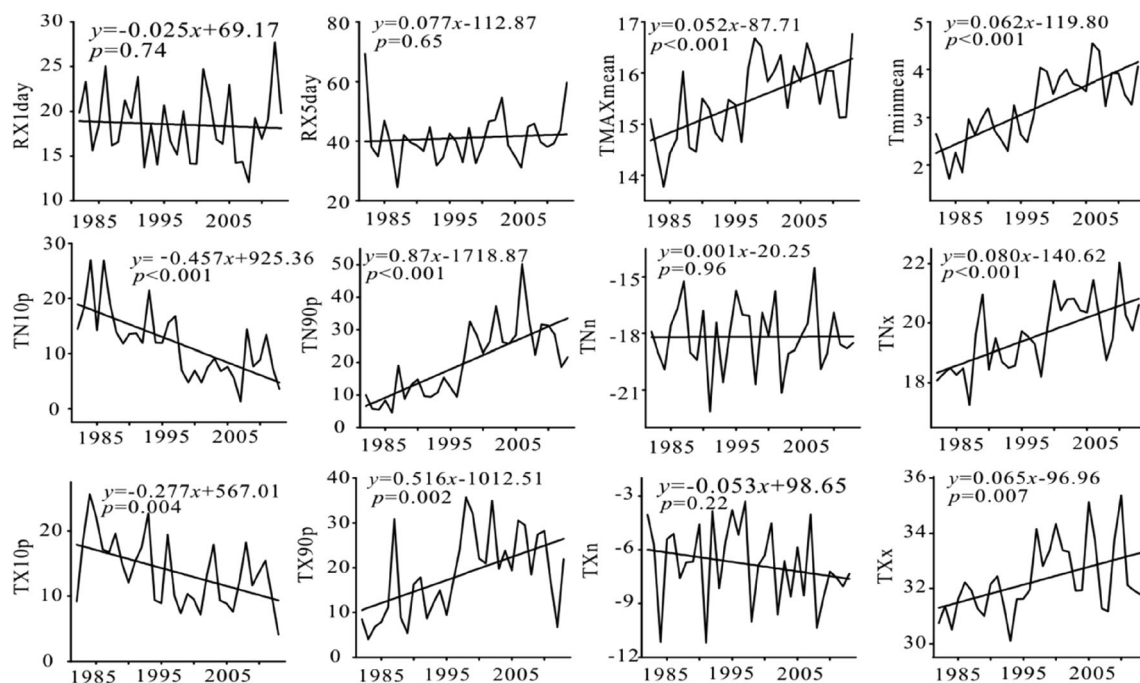


Fig. 4 Liner trend in climate extreme indices in the LP during 1982–2013

Table 2 Correlations between NDVI and climate extreme indices on yearly time scale, 1982–2013

	RX1day	RX5day	TMAXmean	TMINmean	TN10p	TN90p
NDVI	0.141	0.108	0.235	0.351*	-0.321	0.241
	TNn	TNx	TX10p	TX90p	TXn	TXx
NDVI	-0.155	0.316	-0.235	0.107	-0.290	0.154

Note: *, **Means significant at $P = 0.05$ and 0.01

farmland, and forest could be explained by RX5day. The strongest correlations were found between all the vegetation types and extreme temperature indicators (TMAXmean, TMINmean, TNn, TNx, TXn, and TXx) ($P < 0.01$). For example, TMINmean explained 84, 88, 89, and 89% of the vegetation dynamics in grassland, shrub land, farmland, and forest, respectively.

Considering that vegetation responds differently to climate extremes in different seasons, the correlations between NDVI and the climate extreme indices for different seasons were calculated (Table 3). All of the precipitation extremes (RX1day and RX5day) and temperature extremes (TMAXmean, TMINmean, TNn, TNx, TXn, and TXx) exhibited significant positive relationships with NDVI in the spring and autumn ($P < 0.01$). However, relationships between NDVI and RX1day, TMAXmean, TXn, and TXx were not

significant in summer, and none of the correlations between NDVI and the temperature extremes were significant in winter. NDVI exhibited significant negative relationships with precipitation extremes (RX1day and RX5day) in winter ($P < 0.05$) (Table 4).

The spatial distribution of the correlations between vegetation and climate extreme indices across different seasons was evaluated (Fig. 6). In spring and autumn, the correlations between vegetation and precipitation and temperature extremes were significantly positive at most of the meteorological stations, except for the Lijin station, and the vegetation in the western region was more strongly correlated with precipitation extremes (Figs. 6, 7, and 8). In summer, there were positive correlations between vegetation and precipitation extremes at 98.08% of the meteorological stations, but only 42.31 and 63.46% meteorological stations had significant positive correlations ($P < 0.05$). For the temperature extremes, 26.92, 92.31, 90.39, 94.23, 76.92, and 17.31% of the meteorological stations exhibited positive correlations between vegetation and TMAXmean, TMINmean, TNn, TNx, TXn, and TXx, but of those, only 11.54, 65.39, 57.69, 36.54, 17.31, and 9.62% were significantly positive ($P < 0.05$), which were distributed mainly in the northwest region of the LP (Fig. 7). In winter, 3.85% of the meteorological stations had positive correlations between vegetation and precipitation extremes, and none of the correlations were significant correlation. For

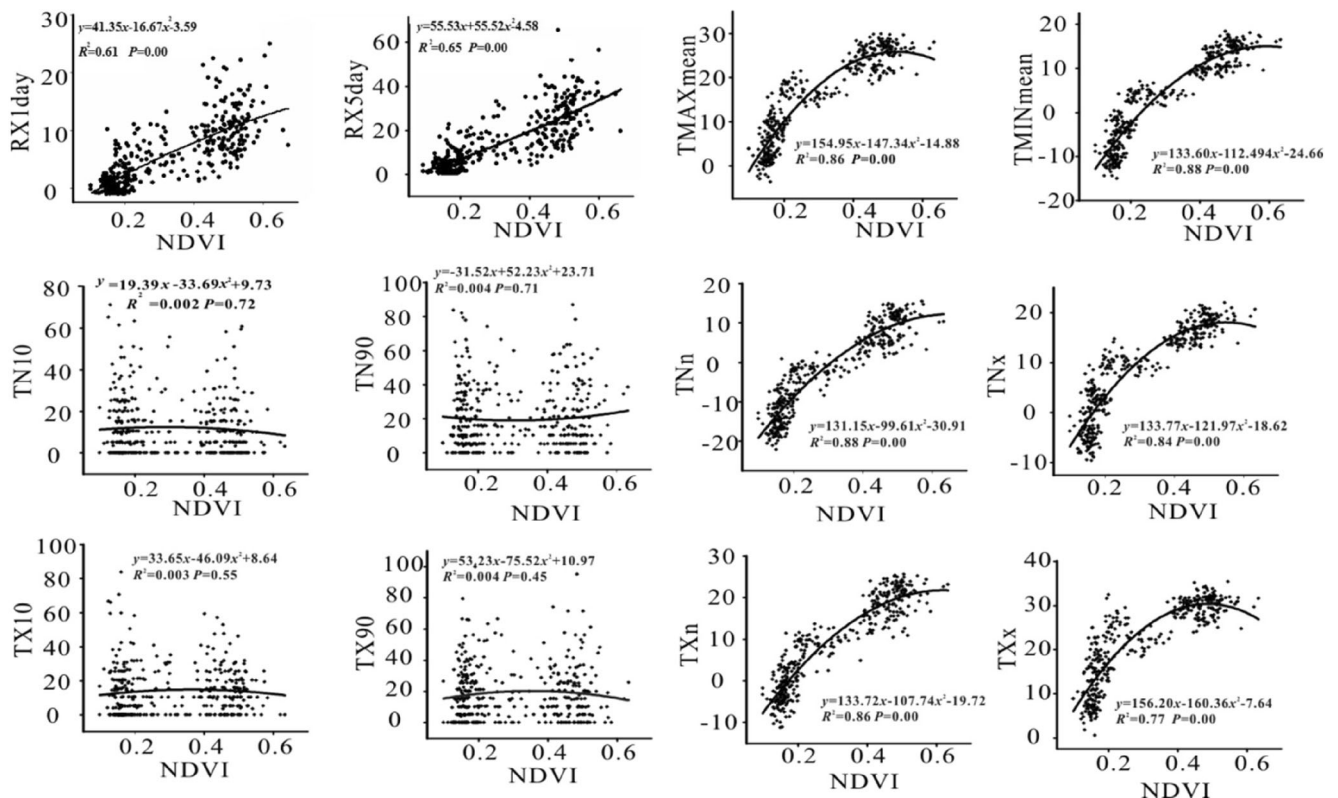


Fig. 5 Correlations between NDVI and climate extreme indices on monthly time scale, 1982–2013

Table 3 Regression analysis between NDVI and selected ten climate extreme indices for different vegetation types

	Grassland	Shrub land	Farmland	Forest
RX1day	$y = -0.0007x^2 + 0.030x + 0.087 R^2 = 0.64$	$y = -0.0012x^2 + 0.048x + 0.148 R^2 = 0.67$	$y = -0.0009x^2 + 0.038x + 0.126 R^2 = 0.66$	$y = -0.0013x^2 + 0.053x + 0.239 R^2 = 0.67$
RX5day	$y = -0.0001x^2 + 0.014x + 0.089 R^2 = 0.70$	$y = -0.0002x^2 + 0.0322x + 0.154 R^2 = 0.71$	$y = -0.0002x^2 + 0.018x + 0.131 R^2 = 0.72$	$y = -0.0003x^2 + 0.025x + 0.247 R^2 = 0.70$
TMAXmean	$y = -196.55x^2 + 170.69x - 11.08 R^2 = 0.81$	$y = -73.45x^2 + 106.49x - 12.24 R^2 = 0.86$	$y = -133.59x^2 + 148.24x - 15.22 R^2 = 0.876$	$y = -46.51x^2 + 91.83x - 16.96 R^2 = 0.88$
TMINmean	$y = -154.87x^2 + 150.59x - 21.62 R^2 = 0.84$	$y = -53.20x^2 + 92.71x - 22.20 R^2 = 0.88$	$y = -103.62x^2 + 128.9x - 25.11 R^2 = 0.89$	$y = -33.46x^2 + 78.99x - 26.62 R^2 = 0.89$
TNn	$y = -149.64x^2 + 154.79x - 28.53 R^2 = 0.84$	$y = 51.34x - 22.43 R^2 = 0.87$	$y = -94.06x^2 + 1127.95x - 31.54 R^2 = 0.89$	$y = 49.05x - 26.90 R^2 = 0.88$
TNx	$y = -153.51x^2 + 142.84x - 14.85 R^2 = 0.80$	$y = -65.46x^2 + 96.13x - 16.98 R^2 = 0.84$	$y = -111.66x^2 + 128.76x - 19.03 R^2 = 0.86$	$y = -49.97x^2 + 91.51x - 23.07 R^2 = 0.86$
TXn	$y = -162.58x^2 + 158.45x - 17.41 R^2 = 0.83$	$y = 49.3x - 10.58 R^2 = 0.86$	$y = -99.55x^2 + 129.06x - 20.15 R^2 = 0.87$	$y = 47.33x - 14.99 R^2 = 0.87$
TXx	$y = -198.57x^2 + 163.18x - 2.99 R^2 = 0.71$	$y = -86.56x^2 + 111.65x - 5.64 R^2 = 0.76$	$y = -145.36x^2 + 149.56x - 8.01 R^2 = 0.79$	$y = -63.48x^2 + 103.99x - 11.98 R^2 = 0.79$

Note: *, **Means significant at $P = 0.05$ and 0.01

Table 4 Correlations between NDVI and selected ten climate extreme indices for different seasons

	Spring	Summer	Autumn	Winter
RX1day	0.552**	0.181	0.674**	-0.302**
RX5day	0.628**	0.296**	0.721**	-0.355**
TMAXmean	0.860**	0.064	0.923**	0.168
TMINmean	0.898**	0.480**	0.935**	0.002
TNn	0.874**	0.345**	0.900**	0.069
TNx	0.833**	0.466**	0.913**	-0.088
TXn	0.858**	0.199	0.876**	0.094
TXx	0.741**	0.005	0.879**	0.091

Note: **Means significant at $P = 0.01$

the temperature extremes, 86.54, 42.31, 40.39, 30.77, 86.54, and 73.08% of the meteorological stations exhibited positive correlations between vegetation and TMAXmean, TMINmean, TNn, TNx, TXn, and TXx, but of those, only 28.85, 7.69, 3.85, 3.85, 5.77, and 23.08% were significantly positive ($P < 0.05$) (Fig. 9).

3.5 Correlation of vegetation and ecological restoration activities

Human activities have also been major driving forces in the LP, and the GGP was implemented in 1999 to control water loss and soil erosion (Lü et al. 2012). This project may have been played a key role in vegetation recovery during recent decades. In 2003, cultivated vegetation was converted to forest and grassland in Shaanxi over 5000 km², and 3000 km² of afforestation was planted in Ningxia and Shanxi (Xiao 2014). Because of the GGP, afforested areas of Shaanxi, Shanxi, and Ningxia accounted for 15–20% of the national afforested area in most years, especially in 1999, with the three provinces accounting for 55.7% of the national afforested area. In 1999–2012, the total afforested area of the three provinces reached 3.8×10^4 km² (Xiao 2014). This indicates that the efforts of the GGP have been generally effective in the LP, the pilot region of the program. In this study, vegetation cover in the pilot regions for ecological restoration (Yulin and Yan'an) exhibited an overall improvement since the implementation of the GGP. A strong correlation between NDVI and the cumulative afforestation areas was detected during 1998–2013, at $r = 0.859$ and 0.85 , $n = 16$, $P < 0.001$ (Fig. 10). During the last decades, the LP experienced severe water loss and soil erosion and produced a high yield of coarse sediment. However, the sediment transfer from this region to the Yellow River declined from 1.6 to 0.14 billion tons during the recent decade (Zhao et al. 2013). Therefore, it is suggested that the GGP has been largely responsible for vegetation greening and the control of soil and water losses.

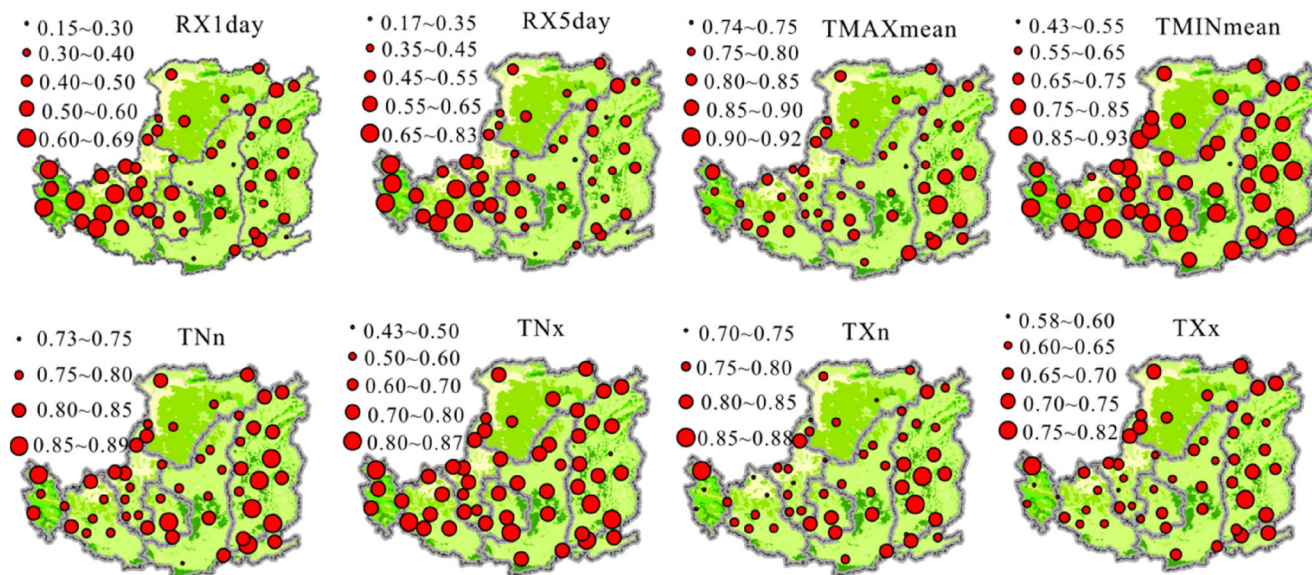


Fig. 6 Spatial distributions of correlations between vegetation and extreme indices in spring

4 Discussion

Our results show a significant increasing trend (0.025/10a) for the NDVI in the LP from 1982 to 2013, which is consistent with previous studies (Sun et al. 2015a, b; Zhang et al. 2013a, b). This change rate is larger than the change rate in China (0.007/10a from 1982 to 2011) (Liu and Lei 2015), and it is also larger than the Tibetan Plateau (0.004/10a from 1982 to 2012) (Du et al. 2016). For the change of climate extreme indices, our results show a significant increasing trend (0.52 °C/10a, 0.62 °C/10a, 8.7 days/10a, 0.80 °C/10a, 5.16 days/10a, and 0.65 °C/10a) for TMAXmean, TMINmean, TN90p, TNx, TX90p, and TXx. Our seasonal results are consistent with previous studies (Sun et al. 2016; Zhao et al. 2016).

For the correlations between vegetation and climate extreme indices, our results indicated that certain climate extreme indices (RX1day, RX5day, TMAXmean, TMINmean, TNn, TNx, TXn, and TXx) had stronger impacts on vegetation at the monthly time scale in the LP. The relationships between vegetation and climate extreme indices also varied with seasons. This result is consistent with findings from Tan et al. (2015). The correlations between vegetation and climate extreme indices were stronger in spring and autumn than in summer and winter (Table 4). The efficiency of water use and plant photosynthesis with temperature increase promotes the growth of vegetation in spring (Tan et al. 2015). Plant metabolism weakens as the available energy decrease in autumn. In summer, high temperatures may lead to a decline in soil moisture and an increase in evaporation. Rainfall is concentrated

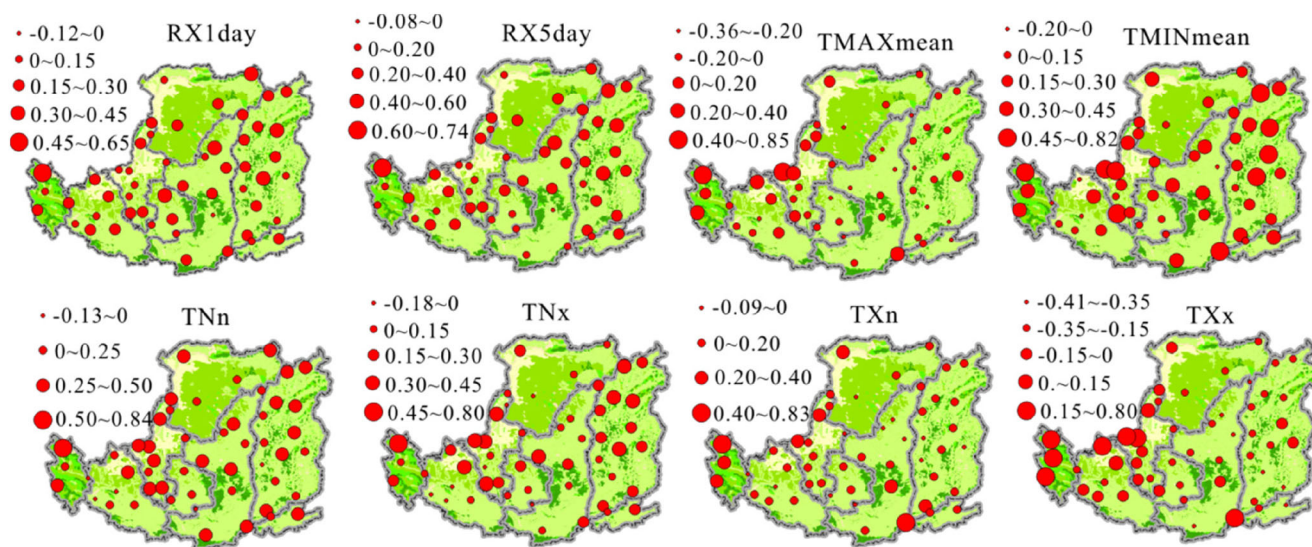


Fig. 7 Spatial distributions of correlations between vegetation and extreme indices in summer

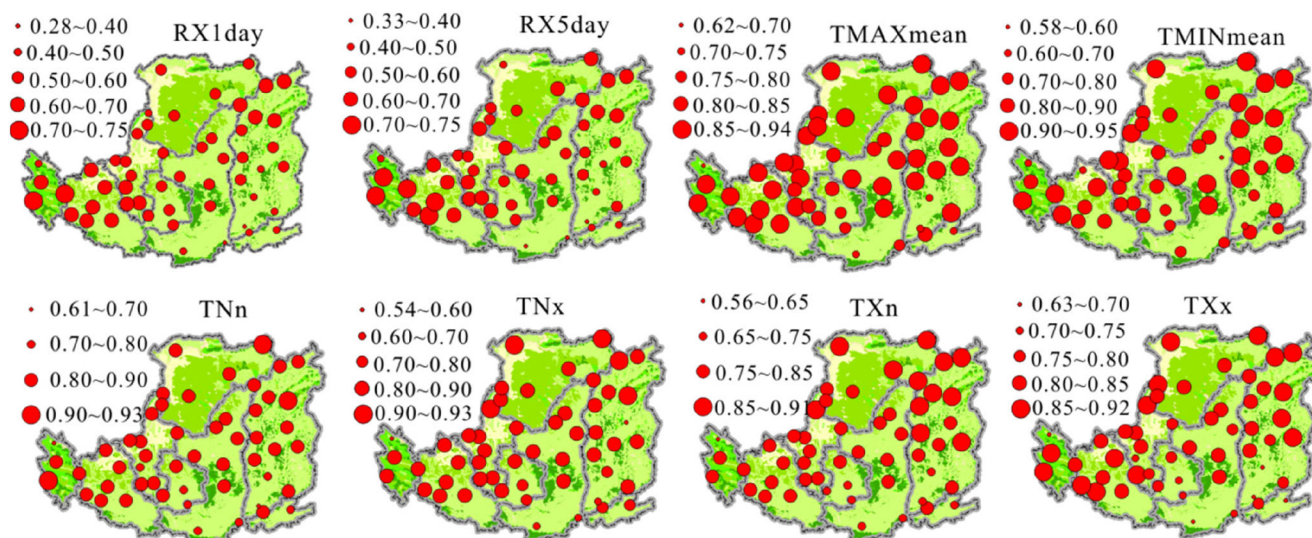


Fig. 8 Spatial distributions of correlations between vegetation and extreme indices in autumn

mainly in the summer in the LP, and frequent heavy precipitation events have considerable impacts on agriculture and soil erosion (Sun et al. 2016), which are not beneficial to the growth of vegetation. In winter, deciduous forest and annual herbaceous vegetation coverage decreases due to phenological features rather than climate change (Tan et al. 2015). The negative correlations between extreme precipitation indices (RX1day and RX5day) and monthly NDVI values imply that an increase in precipitation could cause a decrease of NDVI in winter. Soil temperature would decrease with precipitation, and soil temperature would probably become a key constraining factor for vegetation growth (Zhang et al. 2013a, b).

In addition, human activities also play the important role in the vegetation growth in the LP. In 1999, the Chinese government implemented a nationwide ecological recovery program

the GGP, and approximately US \$8.7 billion has been invested to convert previously farmed lands to perennial non-native vegetation (Feng et al. 2016). Though the GGP, 16,000 km² of rain-fed cropland was converted to artificial vegetation (Feng et al. 2016), causing a 21% increase in vegetation cover from 1999 to 2013 (Fig. 2a). Both forestry statistics and satellite-derived continuous fields indicated that vegetation cover on the LP has almost doubled and sediment discharge into the Yellow River has declined from 1999 to 2013 (Chen et al. 2015). As result of GGP, ecosystem services also improved on the LP from 2000 to 2010 (Ouyang et al. 2016). The strong correlation between NDVI and cumulative afforestation indicated that the increase in vegetation cover was driven by the GGP (Fig. 10). Previous modeling studies have also indicated that the GGP-enhanced carbon stocks in biomass and soils in the LP (Chang et al. 2011; Liu et al. 2014).

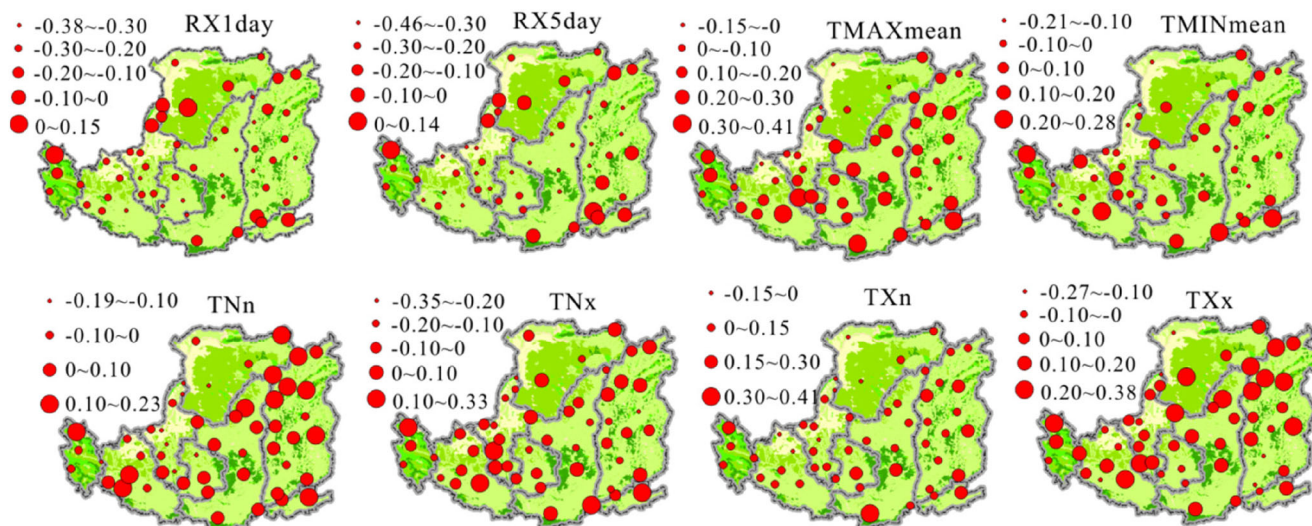


Fig. 9 Spatial distributions of correlations between vegetation and extreme indices in winter

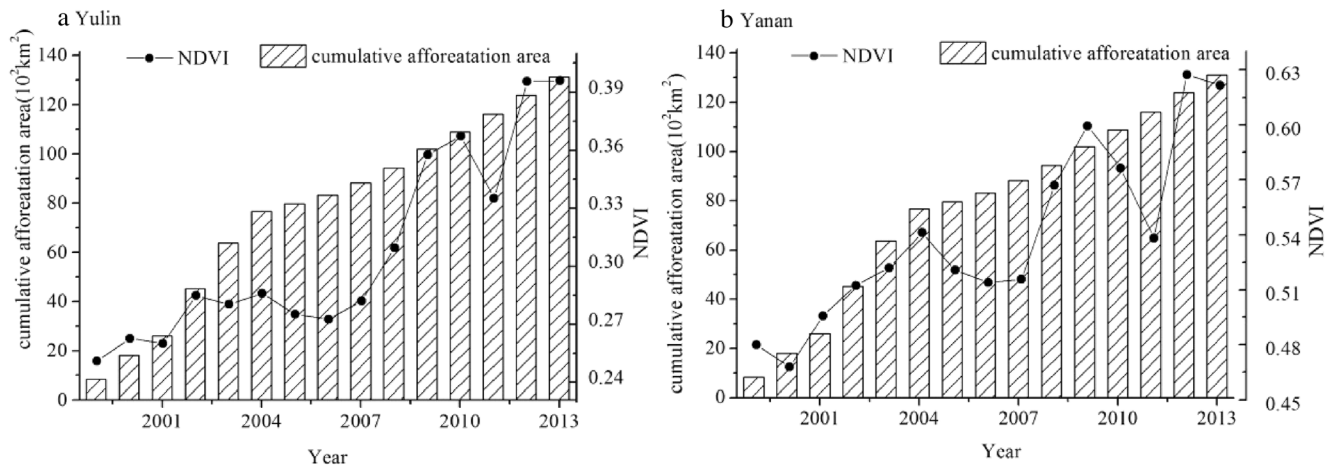


Fig. 10 Correlation of cumulative afforestation with growing season NDVI

This showed that the effort in converting croplands on steep slopes to grassland or forests has been generally effective in the LP. However, the new planting has caused increased evapotranspiration (ET) and resulted in water shortages, artificial forest, and grassland degradation in the arid and semi-arid regions (Cao et al. 2011). Statistics indicated that the overall survival rate of artificial forest from 1982 to 2005 was only 24%, and much of the artificial forest in the LP was made up of “small but old trees” because of the soil water deficit (Wang et al. 2007). Therefore, an excessive reliance on afforestation in arid and semi-arid regions is risky, and farming and grazing, natural rehabilitation, and other non-intensive conversion activities should be emphasized in current and future ecological restoration projects in the LP (Sun et al. 2015a, b).

The correlations between some of the extreme climate indices and vegetation coverage may help identify vulnerable ecosystems under climate extremes in this area. However, the spatial resolution of the AVHRR NDVI3g is coarse, and there were a small number of available meteorological stations in our study. Meanwhile, the time-lag effects of extreme climate indices on variability in vegetation growth were not detected in this study. Therefore, our results may reflect only general vegetation coverage dynamics in response to extreme climate indices; more spatial information on the response of vegetation dynamics to extreme climate indices needs to be analyzed in the future. Previous studies have suggested that climate datasets with high spatial resolutions may provide an efficient way to describe the spatial and temporal vegetation changes associated with extreme climate indices and climate change. Such analysis could provide interesting insights if applied within the LP (Sillmann et al. 2013; Hu et al. 2014). Multisensor NDVI datasets have been used widely in local to global scale modeling and analysis, but the outcomes of these studies suggest that there is considerable bias in multisensor NDVI records (Tarnavsky et al. 2008). In this

study, we used the longest global time series of vegetation dynamics and indicated that the overall trend has improved in the LP. However, the spatial resolutions of the AVHRR NDVI3g were coarse, and the number of available meteorological stations was limited in our study. Moderate Resolution Imaging and Spectroradiometer (MODIS NDVI) is also considered to be an improvement over the NDVI product. Previous studies showed that the trends of GIMMS NDVI were similar to MODIS NDVI data for the Northern Hemisphere areas except for high arctic regions. Fensholt and Proud (2012) assessed the quality of the GIMMS3g NDVI data against MODIS NDVI using pixel wise linear regression analysis. Results indicated that trends of GIMMS NDVI in overall acceptable agreement with MODIS NDVI data during 2000–2010. Zhang et al. (2016a, b) investigated the effectiveness of ecological restoration programs on vegetation activities in the “Three North” region over the past three decades, using the NDVI from GIMMS3g and MODIS. Results indicated the increasing trend of greenness in the Three North region. Our results may reflect only general vegetation coverage dynamics; the relationships between MODIS NDVI and climate extremes need to be analyzed in the future. Nevertheless, although this study does suffer from the aforementioned drawbacks, our findings are still meaningful for understanding the change trends of climate extreme and how they impact vegetation growth, for use in implementing an ecological recovery program and improving the knowledge of vegetation vulnerability to extreme climate change and variability.

5 Conclusions

This study analyzed change trends for vegetation cover and the vegetation response to climate extremes in the LP of

Central China from 1982 to 2013. The major conclusions are summarized as follows:

(a) Vegetation cover in the LP exhibited significant linear increase at a rate of 0.025/10a ($P < 0.001$) from 1982 to 2013. A sharp increase occurred after 1999 (rate of 0.08/10a) in the LP. As for spatial the distribution, NDVI values showed an increasing trend from northwest to southeast, with about 61.79% of the region exhibited a significant increasing trend ($P < 0.05$).

(b) The indices TMAXmean, TMINmean, TN90p, TNx, TX90p, and TXx all increased significantly at rates of 0.77 mm/10a, 0.52 °C/10a, 0.62 °C/10a, 0.80 °C/10a, 5.16 days/10a, and 0.65 °C/10a, respectively. On the contrary, TX0p and TN10p index values decreased significantly at rates of 2.77 days/10a and 4.57 days/10a ($P < 0.01$), respectively.

(c) Ecological restoration programs may have played a key role in vegetation recovery throughout the LP from 1998 to 2013. And the relationship between NDVI and extreme temperature index (TMINmean) at nighttime is significant yearly time scale. Correlation analysis found that vegetation coverage and vegetation types responded significantly positively to RX5day, RX1day, TMAXmean, TMINmean, TNx, TNn, TXn, and TXx at the monthly time scale ($P < 0.01$).

(d) All of the precipitation and temperature extremes exhibited significantly positive relationships with NDVI in the spring and autumn ($P < 0.01$). However, the relationships between NDVI and RX1day, TMAXmean, TXn, and TXx were not significant in summer. In winter, vegetation exhibited a significantly negative relationship with precipitation extremes ($P < 0.05$).

Acknowledgments The work was partially supported by the Natural Science Foundation of Hebei Province (Grant # D2015402134), Education Department of Hebei Province (Grant YQ2013012, QN 2014184), and National High Technology Research and Development Program 863 of China (Grant # 2015AA123901).

References

- Cao SX, Chen L, Shankman D, Wang CM, Wang XB, Zhang H (2011) Excessive reliance on afforestation in China's arid and semi-arid regions: lessons in ecological restoration. *Earth-Sci Rev* 104:240–245. doi:10.1016/j.earscirev.2010.11.002
- Chang RY, Fu BJ, Liu GH, Liu SG (2011) Soil carbon sequestration potential for “grain for green” project in loess Plateau, China. *Environ Manag* 48(6):1158–1172. doi:10.1007/s00267-011-9682-8
- Chen YP, Wang KB, Lin YS, Shi WY, Song Y, He XH (2015) Balancing green and grain trade. *Nat Geosci* 8:739–741. doi:10.1038/geo2544
- Du JQ, Shu JM, Yin JQ, Yuan XJ, Jiaerheng A, Xiong SS, He P, Liu WL (2015) Analysis on spatiotemporal trends and drivers in vegetation growth during recent decades in Xinjiang, China. *Int J Appl Earth Obs* 38:216–228. doi:10.1016/j.jag.2015.01.006
- Du JQ, Zhao CX, Shu JM, Jiaerheng A, Yuan XJ, Yin JQ, Fang SF, He P (2016) Spatiotemporal changes of vegetation on the Tibetan Plateau and relationship to climatic variables during multiyear periods from 1982–2012. *Environ Earth Sci* 75(1):1–18. doi:10.1007/s12665-015-4818-4
- Feng XM, Fu BJ, Piao SL, Wang S, Ciais P, Zeng ZZ, Lü YH, Zeng Y, Li Y, Jiang XH, Wu BF (2016) Revegetation in China's loess Plateau is approaching sustainable water resource limits. *Nat Clim Chang* 6:1019–1022. doi:10.1038/NCLIMATE3092
- Fensholt R, Proud SR (2012) Evaluation of Earth observation based global long term vegetation trends - comparing GIMMS and MODIS global NDVI time series. *Remote Sens Environ* 119:131–147. doi:10.1016/j.rse.2011.12.015
- Guay KC, Beck P, Berner LT, Goetz SJ, Baccini A, Buermann W (2014) Vegetation productivity patterns at high northern latitudes: a multi-sensor satellite data assessment. *Glob Chang Biol* 20:3147–3158. doi:10.1111/gcb.12647
- Hilker T, Lyapustin AI, Tucker CJ, Hall FG, Myneni RB, Wang YJ, Bi J, de Moura YM, Sellers PJ (2014) Vegetation dynamics and rainfall sensitivity of the Amazon. *P Natl Acad Sci USA* 111:16041–16046. doi:10.1073/pnas.1404870111
- Hou X (2001) Vegetation atlas of China. Chinese academy of Science, the editorial Board of Vegetation map of China. Beijing, China, scientific press.
- Hu ZY, Zhang C, Hu Q, Tian HQ (2014) Temperature changes in Central Asia from 1979 to 2011 based on multiple datasets. *J Clim* 27:1143–1167. doi:10.1175/JCLI-D-13-00064.1
- John R, Chen JQ, Ou-Yang ZT, Xiao JF, Becker R, Samanta A, Ganguly S, Yuan WP, Batkhishig O (2013) Vegetation response to extreme climate events on the Mongolian Plateau from 2000 to 2010. *Environ Res Lett* 8(UNSP 0350333). doi: 10.1088/1748-9326/8/3/035033
- Li Z, Zheng FL, Liu WZ, Flanagan DC (2010) Spatial distribution and temporal trends of extreme temperature and precipitation events on the loess Plateau of China during 1961–2007. *Quatern Int* 226:92–100. doi:10.1016/j.quaint.2010.03.003
- Li Z, Zheng FL, Liu WZ (2012) Spatiotemporal characteristics of reference evapotranspiration during 1961–2009 and its projected changes during 2011–2099 on the loess Plateau of China. *Agric For Meteorol* 154:147–155. doi:10.1016/j.agrformet.2011.10.019
- Liao H, Chang WY (2014) Integrated assessment of air quality and climate change for policy-making: highlights of IPCC AR5 and research challenges. *Natl Sci Rev* 1:176–179. doi:10.1093/nsr/nwu005
- Liu Y, Lei H (2015) Responses of natural vegetation dynamics to climate drivers in China from 1982 to 2011. *Remote Sens-Basel* 7(8):10243–10268. doi:10.3390/rs70810243
- Liu G, Liu HY, Yin Y (2013) Global patterns of NDVI-indicated vegetation extremes and their sensitivity to climate extremes. *Environ Res Lett* 8(0250092). doi:10.1088/1748-9326/8/2/025009
- Liu D, Chen Y, Cai WW, Dong WJ, Xiao JF, Chen JQ, Zhang HC, Xia JZ, Yuan WP (2014) The contribution of China's grain to green program to carbon sequestration. *Landsc Ecol* 29(10):1675–1688. doi:10.1007/s10980-014-0081-4
- Liu XF, Zhu XF, Pan YZ, Zhao AZ, Li YZ (2015a) Spatiotemporal changes of cold surges in Inner Mongolia between 1960 and 2012. *J Geogr Sci* 25:259–273. doi:10.1007/s11442-015-1166-y
- Liu YX, Liu XF, Hu YN, Li SS, Peng J, Wang YL (2015b) Analyzing nonlinear variations in terrestrial vegetation in China during 1982–2012. *Environ Monit Assess* 187(72211). doi:10.1007/s10661-015-4922-7
- Liu XF, Zhu XF, Pan YZ, Li SS, Ma YQ, Nie J (2016) Vegetation dynamics in Qinling-Daba Mountains in relation to climate factors between 2000 and 2014. *J Geogr Sci* 26(1):45–58. doi:10.1007/s11442-016-1253-8
- Lü YH, Fu BJ, Feng XM, Zeng Y, Liu Y, Chang RY, Sun G, Wu BF (2012) A policy-driven large scale ecological restoration: quantifying ecosystem services changes in the loess Plateau of China. *PLoS One* 7(e317822). doi:10.1371/journal.pone.0031782

- Lü YH, Zhang LW, Feng XM, Zeng Y, Fu BJ, Yao XL, Li JR, Wu BF (2015) Recent ecological transitions in China: greening, browning, and influential factors. *Sci Rep-UK* 5(8732). doi:10.1038/srep08732
- Miao CY, Yang L, Chen XH, Gao Y (2012) The vegetation cover dynamics (1982–2006) in different erosion regions of the Yellow River basin, China. *Land Degrad Dev* 23:62–71. doi:10.1002/ldr.1050
- Ouyang ZY, Zheng H, Xiao Y, Polasky S, Liu JG, Xu WH, Wang Q, Zhang L, Yang X, Rao EM, Jiang L, Lu F, Wang XK, Yang GB, Gong SH, Wu BF, Zeng Y, Yang WC, Daily G (2016) Improvements in ecosystem services from investments in natural capital. *Science* 352(6292):1455–1459. doi:10.1126/science.aaf2295
- Peng J, Liu ZH, Liu YH, Wu JS, Han YA (2012) Trend analysis of vegetation dynamics in Qinghai-Tibet Plateau using Hurst exponent. *Ecol Indic* 14:28–39. doi:10.1016/j.ecolind.2011.08.011
- Piao SL, Wang XH, Ciais P, Zhu WT, Liu J (2011) Changes in satellite-derived vegetation growth trend in temperate and boreal Eurasia from 1982 to 2006. *Glob Chang Biol* 17:3228–3239. doi:10.1111/j.1365-2486.2011.02419.x
- Pinzon JE, Tucker CJ (2014) A non-stationary 1981–2012 AVHRR NDVI3g time series. *Remote Sens-Basel* 6:6929–6960. doi:10.3390/rs6086929
- Reichstein M, Bahn M, Ciais P, Frank D, Mahecha MD, Seneviratne SI, Zscheischler J, Beer C, Buchmann N, Frank DC, Papale D, Rammig A, Smith P, Thonicke K, van der Velde M, Vicca S, Walz A, Wattenbach M (2013) Climate extremes and the carbon cycle. *Nature* 500:287–295. doi:10.1038/nature12350
- Seneviratne SI, Nicholls N, Easterling D, Goodess CM (2012) Changes in climate extremes and their impacts on the natural physical environment. *Managing the risks of extreme events and disasters to advance climate change adaptation*: 109–230
- Sillmann J, Kharin VV, Zwiers FW, Zhang X, Bronaugh D (2013) Climate extremes indices in the CMIP5 multimodel ensemble: part 2. Future climate projections *J Geophys Res Atmos* 118:2473–2493. doi:10.1002/jgrd.50188
- Stocker DQ. 2013. *Climate change 2013: The Physical Science Basis. Working Group I Contribution to the Fifth Assessment Report of the Intergovernmental Panel on Climate Change, Summary for Policymakers. IPCC*
- Stow D, Daeschner S, Hope A, Douglas D, Petersen A, Myneni R, Zhou L, Oechel W (2003) Variability of the seasonally integrated normalized difference vegetation index across the north slope of Alaska in the 1990s. *Int J Remote Sens* 24:1111–1117. doi:10.1080/0143116021000020144
- Sun WC, Song H, Yao XL, Ishidaira H, Xu ZX (2015a) Changes in remotely sensed vegetation growth trend in the Heihe Basin of arid northwestern China. *PLoS One* 10(e01353768). doi:10.1371/journal.pone.0135376
- Sun WY, Song XY, Mu XM, Gao P, Wang F, Zhao GJ (2015b) Spatiotemporal vegetation cover variations associated with climate change and ecological restoration in the loess Plateau. *Agric For Meteorol* 209:87–99. doi:10.1016/j.agrformet.2015.05.002
- Sun WY, Mu XM, Song XY, WuD CAF, Qiu B (2016) Changes in extreme temperature and precipitation events in the loess Plateau (China) during 1960–2013 under global warming. *Atmos Res* 168: 33–48. doi:10.1016/j.atmosres.2015.09.001
- Tan ZQ, Tao H, Jiang JH, Zhang Q (2015) Influences of climate extremes on NDVI (normalized difference vegetation index) in the Poyang Lake Basin, China. *Wetlands* 35:1033–1042. doi:10.1007/s13157-015-0692-9
- Tarnavsky E, Garrigues S, Brown ME (2008) Multiscale geostatistical analysis of AVHRR, SPOT-VGT, and MODIS global NDVI products. *Remote Sens Environ* 112(2):535–549. doi:10.1016/j.rse.2007.05.008
- Wallace JM, Held IM, Thompson D, Trenberth KE, Walsh JE (2014) Global warming and winter weather. *Science* 343:729–730. doi:10.1126/science.343.6172.729
- Wang GY, Innes JL, Lei JF, Dai SY, Wu SW (2007) Ecology - China's forestry reforms. *Science* 318:1556–1557. doi:10.1126/science.1147247
- Xiao JF (2014) Satellite evidence for significant biophysical consequences of the "grain for green" program on the loess Plateau in China. *J Geophys Res Biogeosci* 119:2261–2275. doi:10.1002/2014JG002820
- Xin ZB, Xu JX, Zheng W (2008) Spatiotemporal variations of vegetation cover on the Chinese loess Plateau (1981–2006): impacts of climate changes and human activities. *Sci China Ser D* 51:67–78. doi:10.1007/s11430-007-0137-2
- You QL, Kang SC, Aguilar E, Pepin N, Flügel WA, Yan YP, Xu YW, Zhang YJ, Huang J (2011) Changes in daily climate extremes in China and their connection to the large scale atmospheric circulation during 1961–2003. *Clim Dynam* 36(11–12):2399–2417. doi:10.1007/s00382-009-0735-0
- Zhang XB, Hegerl G, Zwiers FW, Kenyon J (2005) Avoiding inhomogeneity in percentile-based indices of temperature extremes. *J Clim* 18: 1641–1651. doi:10.1175/JCLI3366.1
- Zhang BQ, Wu PT, Zhao XN, Wang YB, Gao XD (2013a) Changes in vegetation condition in areas with different gradients (1980–2010) on the loess Plateau, China. *Environ Earth Sci* 68:2427–2438. doi:10.1007/s12665-012-1927-1
- Zhang YL, Gao JG, Liu LS, Wang ZF, Ding MJ, Yang XC (2013b) NDVI-based vegetation changes and their responses to climate change from 1982 to 2011: a case study in the Koshi River Basin in the middle Himalayas. *Glob Planet Chang* 108:139–148. doi:10.1016/j.gloplacha.2013.06.012
- Zhang Y, Peng CH, Li WZ, Tian LX, Zhu QA, Chen H, Fang XQ, Zhang GL, Liu GB, Mu XM, Li ZB, Li SQ, Yang YZ, Wang J, Xiao XM (2016a) Multiple afforestation programs accelerate the greenness in the 'three north' region of China from 1982 to 2013. *Ecol Indic* 61: 404–412. doi:10.1016/j.ecolind.2015.09.041
- Zhang Y, Zhang CB, Wang ZQ, Chen YZ, Gang CC, An R, Li JL (2016b) Vegetation dynamics and its driving forces from climate change and human activities in the Three-River source region, China from 1982 to 2012. *Sci Total Environ* 563:210–220. doi:10.1016/j.scitotenv.2016.03.223
- Zhao GJ, Mu XM, Tian P, Jiao JY, Wang F (2013) Have conservation measures improved Yellow River health? *J Soil Water Conserv* 68(6):159A–161A. doi:10.2489/jswc.68.6.159A
- Zhao AZ, Liu XF, Zhu XF, Pan YZ, Zhao YL, Wang DL (2016) Trend variations and spatial difference of extreme air temperature events in the loess Plateau from 1965 to 2013. *Geogr Res* 35:639–652. doi:10.11821/dlyj201604004
- Zheng JY, Hao ZX, Fang XQ, Ge QS (2014) Changing characteristics of extreme climate events during past 2000 years in China. *Prog Geo* 33:3–12. doi:10.11820/dlkxjz.2014.01.001